



## Long-term trends in nitrogen oxides concentrations and on-road vehicle emission factors in Copenhagen, London and Stockholm<sup>☆</sup>

Patricia Krecl<sup>a,\*</sup>, Roy M. Harrison<sup>b,c</sup>, Christer Johansson<sup>d</sup>, Admir Créso Targino<sup>a</sup>, David C. Beddows<sup>b</sup>, Thomas Ellermann<sup>e</sup>, Camila Lara<sup>a</sup>, Matthias Ketzel<sup>e,f</sup>

<sup>a</sup> Graduate Program in Environmental Engineering, Federal University of Technology, Av. Pioneiros 3131, 86036-370, Londrina, PR, Brazil

<sup>b</sup> School of Geography, Earth and Environmental Sciences, University of Birmingham, Edgbaston, Birmingham, B15 2TT, United Kingdom

<sup>c</sup> Department of Environmental Sciences, Center of Excellence in Environmental Studies, King Abdulaziz University, PO Box 80203, Jeddah, 21589, Saudi Arabia

<sup>d</sup> Department of Environmental Science, Stockholm University, Svante Arrhenius väg 8, 106 91, Stockholm, Sweden

<sup>e</sup> Department of Environmental Science, Aarhus University, Frederiksborgvej 399, DK-4000, Roskilde, Denmark

<sup>f</sup> Global Centre for Clean Air Research (GCARE), University of Surrey, Guildford, GU2 7XH, United Kingdom

### ARTICLE INFO

#### Keywords:

NO<sub>x</sub>  
Air quality in Europe  
OSPM model  
Road transport  
Dieselization

### ABSTRACT

Road transport is the main anthropogenic source of NO<sub>x</sub> in Europe, affecting human health and ecosystems. Thus, mitigation policies have been implemented to reduce on-road vehicle emissions, particularly through the Euro standard limits. To evaluate the effectiveness of these policies, we calculated NO<sub>2</sub> and NO<sub>x</sub> concentration trends using air quality and meteorological measurements conducted in three European cities over 26 years. These data were also employed to estimate the trends in NO<sub>x</sub> emission factors (EF<sub>NO<sub>x</sub></sub>, based on inverse dispersion modeling) and NO<sub>2</sub>:NO<sub>x</sub> emission ratios for the vehicle fleets under real-world driving conditions. In the period 1998–2017, Copenhagen and Stockholm showed large reductions in both the urban background NO<sub>x</sub> concentrations (−2.1 and −2.6% yr<sup>−1</sup>, respectively) and EF<sub>NO<sub>x</sub></sub> at curbside sites (68 and 43%, respectively), proving the success of the Euro standards in diminishing NO<sub>x</sub> emissions. London presented a modest decrease in urban background NO<sub>x</sub> concentrations (−1.3% yr<sup>−1</sup>), while EF<sub>NO<sub>x</sub></sub> remained rather constant at the curbside site (Marylebone Road) due to the increase in public bus traffic. NO<sub>2</sub> primary emissions—that are not regulated—increased until 2008–2010, which also reflected in the ambient concentrations. This increase was associated with a strong dieselization process and the introduction of new after-treatment technologies that targeted the emission reduction of other species (e.g., greenhouse gases or particulate matter). Thus, while regulations on ambient concentrations of specific species have positive effects on human health, the overall outcomes should be considered before widely adopting them. Emission inventories for the on-road transportation sector should include EF<sub>NO<sub>x</sub></sub> derived from real-world measurements, particularly in urban settings.

### 1. Introduction

Road transport is the main anthropogenic source of nitrogen oxides (NO<sub>x</sub>) on a global scale (23% in 2017, McDuffie et al., 2020) and across Europe (39% in 2017, EEA, 2019). In traffic environments, NO<sub>x</sub> consists mainly of nitric oxide (NO) and nitrogen dioxide (NO<sub>2</sub>), with the latter associated with a series of deleterious health effects (Nathan and Cunningham-Bussell, 2013; Brown, 2015; Atkinson et al., 2018). Moreover, NO<sub>x</sub> affects human health indirectly—through the production of surface ozone (O<sub>3</sub>) (Monks et al., 2015) and secondary inorganic aerosol

(Fuzzi et al., 2015)—and impacts the environment—through eutrophication and acidification of sensitive ecosystems (Peel et al., 2013).

European countries, in particular those in the northwest, have pioneered strategies to tackle environmental issues, with prominent roles in the international community (Lieverink et al., 2009; Grennfelt et al., 2020). In that context, air pollution has been a major political concern in Europe since the late 1970s, leading to the development of ambient air quality standards and control of the major emissions sources (Crippa et al., 2016). In the case of road transport, new vehicles have had to meet increasingly stringent emission limits since the early 1990s, established

<sup>☆</sup> This paper has been recommended for acceptance by Pavlos Kassomenos.

\* Corresponding author.

E-mail address: [patriciak@utfpr.edu.br](mailto:patriciak@utfpr.edu.br) (P. Krecl).

by the so-called ‘Euro emission standards’ (European Commission, 2021). These standards are based on emission factors (EF) measured in laboratories under controlled conditions following regulatory driving cycles.

However, field studies revealed that the EF simulated with traffic emission models (COmputer Programme to calculate Emissions from Road Transport, COPERT, and Handbook Emission Factors for Road Transport, HBEFA), and validated with laboratory-based EF, largely underestimated the real exhaust emissions (Carslaw et al., 2011; Carslaw and Rhys-Tyler, 2013; Krecl et al., 2017). Because laboratory-based EF are used to compile the official national inventories for the road transport sector, it is of utmost importance to conduct real-world EF measurements to identify mismatches in the emission models (Franco et al., 2013). In light of this, the European Union through the Real Driving Emissions mandates that laboratory tests be complemented with real driving condition tests for new passenger cars (PC) and light-commercial vehicles (LCV) since September 2019 (European Commission, 2021). On the other hand, to assess how EF has responded to policies on emission reduction and its long-term trend, we need to consider approaches based on continuous measurements over a long period. In that context, extended datasets of ambient air pollutant concentrations at roadside sites available in several European cities can be used.

In the case of nitrogen species, only NO<sub>x</sub> emissions are regulated for on-road vehicles in Europe, despite NO<sub>2</sub> being also directly emitted by vehicle exhausts (Carslaw et al., 2011). The NO<sub>2</sub>:NO<sub>x</sub> emission ratios largely increased in Europe in the period 1995–2010 (Grange et al., 2017), and the annual air quality standard for NO<sub>2</sub> was still exceeded at 10% of the European stations (329 out of 3260), mainly near roads (European Environmental Agency, 2019). This is particularly worrying since roadside stations are located in densely populated areas where population exposure can be large.

Based on unique long-term datasets, this study analyzed the trends of NO<sub>2</sub> and NO<sub>x</sub> concentrations at three curbside sites in three European cities: Copenhagen, London and Stockholm. Then, EF<sub>NO<sub>x</sub></sub> for the vehicle fleet were determined based on the street increment of the NO<sub>x</sub> concentrations and inverse modeling techniques. The NO<sub>2</sub>:NO<sub>x</sub> vehicles emission ratios were estimated using their respective ambient concentrations as proxies. We compare our EF<sub>NO<sub>x</sub></sub> values for the mixed fleet with EF extracted from databases and remote sensing studies. Finally, the temporal evolutions of EF<sub>NO<sub>x</sub></sub> and primary NO<sub>2</sub> emissions are discussed in relation to regional and local policies applied to mitigate the road transport emissions.

## 2. Methods

### 2.1. Sampling sites and instrumentation

We selected paired street canyon and urban background sites in Copenhagen, London and Stockholm, where long-term hourly NO<sub>x</sub> (NO + NO<sub>2</sub>), O<sub>3</sub> and traffic measurements were available. Another criterion was the availability of meteorological data at stations representative of winds above the corresponding street canyons (Table 1, and Supplementary Material). NO<sub>x</sub> and O<sub>3</sub> concentrations were measured using chemiluminescence and ultraviolet photometry analyzers, respectively, complying with European reference methods (EN14211, 2012; EN14625, 2012). Note that the measurements conducted at the air pollution and meteorological sites are subject to rigorous quality assurance procedures since they belong to national networks.

Hourly traffic data consisted of traffic volume (TR) and vehicle speed (VS). Traffic measurements were continuously recorded on Hornsgatan St. (Stockholm) (Krecl et al., 2017) and Marylebone Road (London) (Harrison et al., 2011) by using loop-profilers embedded in the surface. In the case of Jagtvej St. (Copenhagen), pre-defined traffic data profiles provided by the Danish Operational Street Pollution model (OSPM) were scaled up by the annual average daily traffic (AADT) and mean vehicle

**Table 1**

Details of the sites and datasets used in this study.

City	Site	Type	Variables	Period
Copenhagen	Jagtvej	Street canyon	NO <sub>x</sub> , NO <sub>2</sub> , TR, VS	1994–2017
	H.C. Ørsted	Urban background	NO <sub>x</sub> , NO <sub>2</sub> , O <sub>3</sub>	
	H.C. Ørsted	Meteorology	T, RH, WS, WD	
London	Marylebone Road	Street canyon	NO <sub>x</sub> , NO <sub>2</sub> , TR, VS	1998–2017
	North Kensington	Urban background	NO <sub>x</sub> , NO <sub>2</sub> , O <sub>3</sub>	
	Heathrow	Meteorology	T, RH, P, WS, WD	
Stockholm	Hornsgatan	Street canyon	NO <sub>x</sub> , NO <sub>2</sub> , TR, VS	1992–2017
	Torkel	Urban background	NO <sub>x</sub> , NO <sub>2</sub> , O <sub>3</sub>	
	Högdalen	Meteorology	T, P, WS, WD	

T: air temperature, RH: relative humidity, WS: wind speed, WD: wind direction, P: atmospheric pressure.

speed as described in the Supplementary Material, together with details of traffic data validation.

### 2.2. Data processing

#### 2.2.1. Trend analysis of atmospheric concentrations

Trends in air pollutant concentrations can be driven by changes in meteorological conditions, emissions, atmospheric chemistry or the built environment (Grange and Carslaw, 2019; Malley et al., 2018). When trend analysis is conducted for assessing the success of certain air quality management strategies, the influence of the weather conditions on ambient concentrations should be removed. Thus, we applied the *rmweather* R package (version 0.1.51; Grange and Carslaw, 2019) on hourly concentrations measured at all sites to remove this influence. The package builds Random Forest models that predict hourly NO<sub>x</sub> (or NO<sub>2</sub>) concentrations based on several independent variables, and then estimates the meteorologically normalized series. We used the following explanatory variables: Unix date (number of seconds elapsed since Jan. 1, 1970) representing the trend term, Julian day (day of the year) as the seasonal trend, day of the week, hour of the day, and meteorological variables (Table 1). The importance of the predictor variables on the air pollutant concentrations was also assessed with the *rmweather* package. Further details on the model development and normalization technique are given in the Supplementary Material.

The normalized hourly ambient concentrations were aggregated to mean monthly values, which were subsequently used to estimate linear trends by the non-parametric Theil-Sen method (Snell et al., 1996) for each pollutant and site over the common period (1998–2017). The Theil-Sen trend is a median slope trend line resistant to outliers. It was calculated with the *TheilSen* function available in the *openair* R package (Carslaw and Ropkins, 2012), which also computed the confidence intervals at 95% and *p*-values by bootstrap resampling.

#### 2.2.2. Calculation of NO<sub>2</sub>:NO<sub>x</sub> emission ratios

We estimated the NO<sub>2</sub>:NO<sub>x</sub> vehicle emission ratios by filtering ambient concentrations of NO<sub>2</sub> and NO<sub>x</sub> measured at curbside sites following Grange et al. (2017). This technique isolates the primary NO<sub>2</sub> component by selecting measurements conducted in periods when the production of NO<sub>2</sub> via the NO + O<sub>3</sub> reaction is negligible. Thus, we chose only NO<sub>2</sub> and NO<sub>x</sub> concentrations corresponding to traffic-dominated periods (06:00–18:00 on weekdays), with low O<sub>3</sub> background concentrations. An O<sub>3</sub> threshold of 10 µg m<sup>-3</sup> was found appropriate to minimize the NO<sub>2</sub> secondary production and still have enough measurements for the emission ratio calculation (more details are provided in the Supplementary Material). For each curbside site and year combination,

we calculated the slope of the robust linear regression between the filtered NO<sub>x</sub> and NO<sub>2</sub> atmospheric concentrations, which is a proxy of the primary NO<sub>2</sub>:NO<sub>x</sub> emission ratio.

### 2.2.3. Determination of $EF_{NO_x}$

For each street canyon and year, hourly  $EF_{NO_x}$  [ $\text{g veh}^{-1} \text{m}^{-1}$ ] were determined for the mixed fleet as follows (Ketzel et al., 2003; Krecl et al., 2018):

$$EF_{NO_x} = \frac{\Delta NO_x(t) D(t)}{TR(t)}, \quad (1)$$

where  $\Delta NO_x$  [ $\text{g m}^{-3}$ ] is the measured increment concentration (curbside minus urban background concentrations) due to the emissions of vehicles driving on that street,  $TR$  [ $\text{veh s}^{-1}$ ] is the total traffic volume on that street,  $D$  [ $\text{m}^2 \text{s}^{-1}$ ] is the dilution rate and  $t$  is the time [s]. The dilution rate depends on wind conditions, traffic characteristics (TR and VS) and street canyon geometry, and was computed by inverse dispersion modeling using the OSPM (Berkowicz, 2000). Details on the inverse modeling technique can be found elsewhere (Palmgren et al., 1999; Ketzel et al., 2003).

The OSPM has been extensively tested (Kakosimos et al., 2010) and successfully simulates the NO<sub>x</sub> concentrations at regular street canyons, such as Jagtvej and Hornsgatan (Ottosen et al., 2015). However, an initial screening of our OSPM results revealed abnormally high  $D$  values ( $>24 \text{ m}^2 \text{ s}^{-1}$ ) at Marylebone Road site associated with northerly winds with  $WS > 2.0 \text{ m s}^{-1}$ , which we attributed to the more complex street canyon geometry. This wind condition was not very frequent (12%), but may lead to the overestimation of both the dilution and the mean  $EF_{NO_x}$  values if it prevails for certain hours. Thus, these occurrences were excluded from further analysis.

Only hourly  $EF_{NO_x}$  values for the period 07:00–23:00 on weekdays were considered for the analysis because (i) the fleet composition is rather similar between weekdays, and (ii) it avoids the large uncertainties in  $EF_{NO_x}$  calculations associated with the small street increments and low TR, typically observed in the early hours on weekdays (Krecl et al., 2018). Then, mean annual values were calculated for the years displayed in Table 1. Further details on  $EF_{NO_x}$  calculations and OSPM model setup are given in the Supplementary Material.

### 2.2.4. Validation with other databases

The  $EF_{NO_x}$  computed by inverse modeling (Eq. (1)) was compared with  $EF_{NO_x-w}$  calculated by aggregating  $EF_{NO_x i,j,k}$  per vehicle category and weighted according to each category share  $n$  within the fleet, as follows:

$$EF_{NO_x-w} = \sum_{i,j,k} EF_{NO_x i,j,k} \cdot n_{i,j,k}, \quad (2)$$

where the category is a combination of vehicle class  $i$ , fuel  $j$  and Euro standard stage  $k$ .

$EF_{NO_x i,j,k}$  were extracted from three sources: (i) the European Monitoring and Evaluation Program (EMEP) guidebook (EMEP/EEA, 2019), (ii) HBEFA V.3.3 handbook processed for typical site-specific traffic conditions by Burman et al. (2019), and (iii) remote sensing studies conducted under urban driving conditions in Europe (UK: Carslaw et al., 2011; Carslaw and Rhys-Tyler, 2013; Carslaw et al., 2019; Ghaffarpasand et al., 2020, and Sweden: Liu et al., 2019; Zhou et al., 2020) (Table 2). We used the HBEFA  $EF_{NO_x}$  for ethanol and biogas since the other two sources do not include these fuels.

Individual  $EF_{NO_x}$  largely depends on the vehicle category, and the vehicle category share at national and municipal levels can largely differ from the typical share of the actual fleet driving on the canyon street for the same year (Burman et al., 2019). Thus, we profited from the detailed in situ surveys of the vehicle fleet on Hornsgatan St. for the years 2009 and 2017 to validate our  $EF_{NO_x}$  against the EMEP, HBEFA and remote sensing estimates. These surveys analyzed automatic number plate recordings of four million vehicles, and subsequent inquiry of vehicle information from the city municipality provided detailed composition of the fleet in terms of vehicle class, fuel and Euro standard stage (Burman et al., 2019).

## 3. Results and discussion

### 3.1. Trends in ambient concentrations

The most polluted street canyon was Marylebone Road (means of NO<sub>x</sub> and NO<sub>2</sub> in 2017: 286.3 and 83.9  $\mu\text{g m}^{-3}$ ), followed by Hornsgatan (79.9 and 35.3  $\mu\text{g m}^{-3}$ ) and Jagtvej (55.2 and 27.5  $\mu\text{g m}^{-3}$ ). The urban background air was cleanest in Stockholm (means of NO<sub>x</sub> and NO<sub>2</sub> in 2017: 13.3 and 10.7  $\mu\text{g m}^{-3}$ ) followed by Copenhagen (18.4 and 15.3  $\mu\text{g m}^{-3}$ ) and London (50.4 and 32.3  $\mu\text{g m}^{-3}$ ).

Fig. 1 shows the monthly mean NO<sub>x</sub> and NO<sub>2</sub> concentrations measured at the street canyon and urban background sites in Copenhagen (1994–2017), London (1998–2017) and Stockholm (1992–2017), together with the street increments of NO<sub>x</sub> and NO<sub>2</sub> ( $\Delta NO_x$  and  $\Delta NO_2$ , respectively) and the normalized concentrations. Note that the mean NO<sub>2</sub> annual limit of the EU air quality directive (40  $\mu\text{g m}^{-3}$ ) was exceeded every year at the street canyon sites in Copenhagen (1994–2009), London (1998–2017) and Stockholm (1992–2016), and the urban background site in London (1998–2003). The

**Table 2**

Mean  $EF_{NO_x}$  and NO<sub>2</sub>:NO<sub>x</sub> emission ratios for several vehicle categories, taken from remote sensing studies conducted in European cities (UK: Carslaw et al., 2011; Carslaw and Rhys-Tyler, 2013; Carslaw et al., 2019; Ghaffarpasand et al., 2020, and Sweden: Liu et al., 2019; Zhou et al., 2020).

Variable	Euro stage	PC gasoline	PC diesel	LCV diesel	Truck (<12 t) diesel	Truck (>12 t) diesel	<sup>a</sup> Urban bus diesel
$EF_{NO_x}$ [ $\text{g km}^{-1} \text{veh}^{-1}$ ]	E0	2.38	1.22	1.46	5.36	<sup>b</sup> n.a.	n.a.
	E1	1.59	1.24	2.27	3.44	n.a.	11.13
	E2	1.05	1.30	2.01	5.95	13.01	12.35
	E3	0.41	1.23	1.83	5.33	10.61	15.58
	E4	0.23	1.00	1.57	5.09	7.75	16.93
	E5	0.14	1.02	1.86	5.33	7.59	12.78
NO <sub>2</sub> :NO <sub>x</sub> [vol. %]	E0	0.19	0.51	0.67	2.64	0.74	2.40
	E1	3.2	10.8	7.6	6.2	n.a.	n.a.
	E2	2.8	16.8	12.5	11.0	n.a.	11.0
	E3	3.1	8.1	8.4	21.0	11.7	15.4
	E4	4.1	14.9	13.2	12.3	15.8	8.9
	E5	5.6	22.5	23.0	6.2	2.9	8.0
	E6	8.4	18.8	15.5	6.4	4.9	11.3
	E6	10.5	21.7	24.2	15.2	22.5	17.9

<sup>a</sup> A large variation could be observed within the same Euro stage, depending on the after-treatment system (Table S2, Supplementary Material).

<sup>b</sup> Not available.

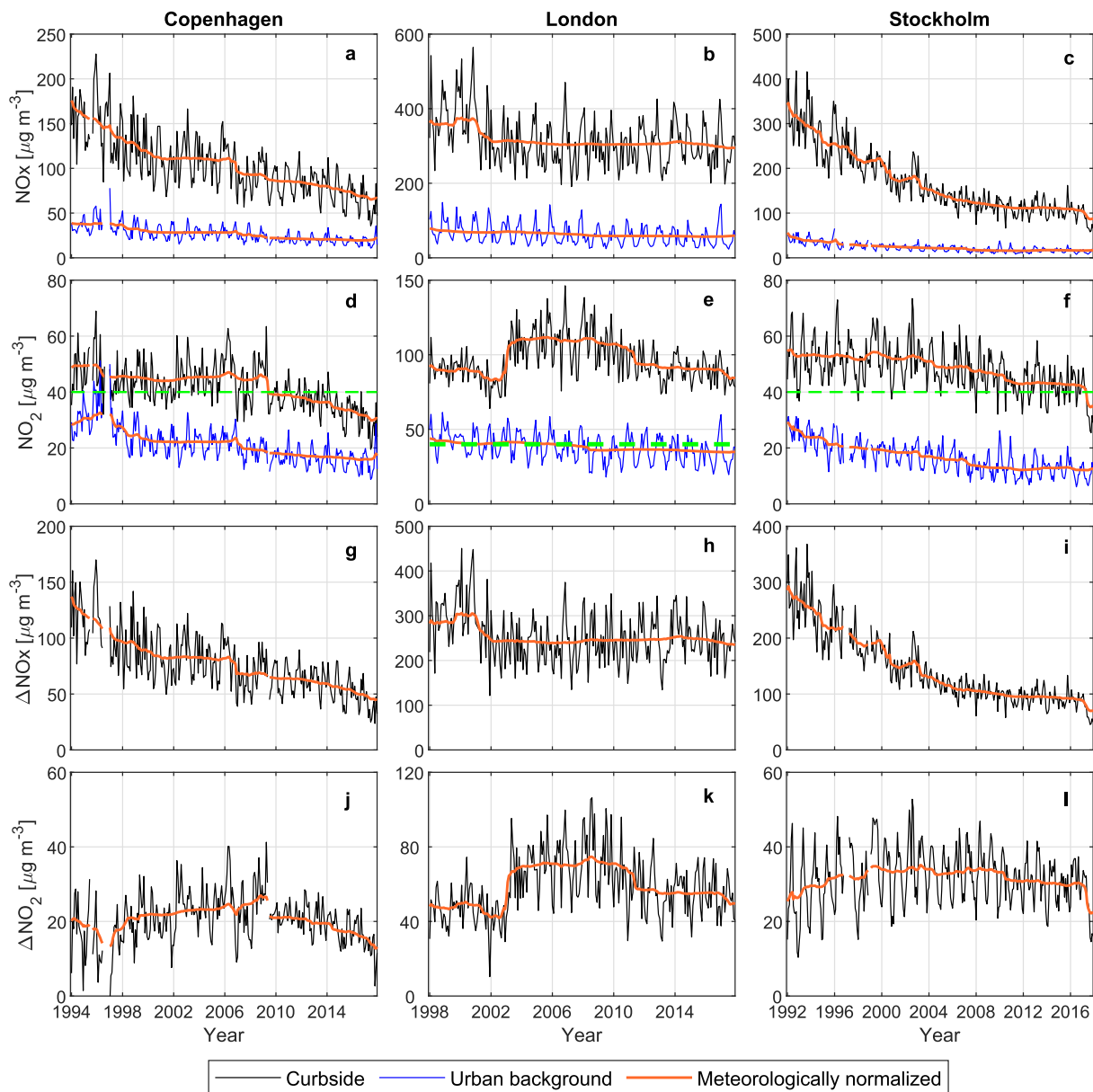


**Fig. 1.** Monthly mean NO<sub>x</sub> and NO<sub>2</sub> concentrations at curbside and urban background sites (a–f), together with NO<sub>x</sub> and NO<sub>2</sub> street increment concentrations (g–l). The orange lines represent the meteorology-normalized concentrations. Note the different y-axis scales adopted to enhance the features in the time series of each site. (For interpretation of the references to colour in this figure legend, the reader is referred to the Web version of this article.)

meteorologically normalized series show a decreasing trend in NO<sub>x</sub>, ΔNO<sub>x</sub> and (to a lesser extent) NO<sub>2</sub> in Stockholm and Copenhagen over the years, but London presented either modest improvements or increase in concentrations at Marylebone Road (Fig. 1a–f). Over the period 1998–2017, Copenhagen and Stockholm showed similar patterns in concentration reductions: (i) NO<sub>x</sub> decreased more at curbside (55–60%) than at urban background sites (41–52%), and (ii) NO<sub>2</sub> reductions were smaller than NO<sub>x</sub>, and declined more at urban background (35–46%) than at street canyon sites (27–35%). London exhibited a different behavior, with the largest NO<sub>x</sub> reduction recorded at the urban background site (36%), and no reductions in NO<sub>2</sub> concentrations at the curbside site (Fig. 1b,e).

Although road transport dominates the total NO<sub>x</sub> emissions in Europe (EEA, 2019), other local and non-local sources might have contributed to ambient NO<sub>x</sub> concentrations at specific sites. Hence, by calculating the NO<sub>x</sub> increment at the street canyon sites the non-local contributions are filtered out, leaving only the traffic-related

contributions from vehicles driving on that street. Street increments for NO<sub>2</sub> and NO<sub>x</sub> were higher for London compared to Stockholm and Copenhagen (Fig. 1g–i), which is consistent with the ADDT values recorded at the canyon streets in the period 1998–2017: 78,300, 27,500 and 18,900 respectively.

In general, the monthly mean concentrations at all sites showed a sawtooth pattern due to meteorologically driven effects on atmospheric mixing and transport and temperature-driven effects on emissions, which were removed after normalization (Fig. 1, orange lines). The analysis of the importance of the explanatory variables of the Random Forest models revealed that the nitrogen oxide concentrations within the street canyons were largely influenced by rooftop-level wind (WD and WS, Fig. S2a, Supplementary Material). This result agrees with Krecl et al. (2015), who reported that recirculation patterns governed the air pollution concentrations within Hornsgatan street canyon (Fig. S2a, Supplementary Material). For example, the site-dependent Random Forest model run in our study was able to capture the recirculation

pattern at that site. The meteorologically normalized concentrations showed non-linear associations with WS, with dilution increasing with WS (e.g., Fig. S2b,d, Supplementary Material). The main predictor for the urban background sites was WS, with high NO<sub>x</sub> concentrations associated with low WS, as also reported by Krecl et al. (2011), while WD had negligible influence. This confirms that the sites can be taken as representative of urban background environment. Kaminska (2019) and Laña et al. (2016) found similar results at other European sites.

In general, seasonal trends played a modest role on NO<sub>x</sub> concentrations, with lower NO<sub>x</sub> values observed in summertime. This is most likely due to improved dispersion and reduced emissions, since summer presents lower traffic volume (long holidays) and higher ambient temperatures might decrease NO<sub>x</sub> emissions for the diesel fleet (Grange et al., 2019).

The trend analysis is very sensitive to the chosen period, as reported by several studies (Grange and Carslaw, 2019; Olstrup et al., 2018). Hence, we focused on the overlapping period 1998–2017 to avoid the influence of site-specific conditions outside these years. Overall, there was a significant downward trend in concentrations (Fig. 2), with NO<sub>x</sub> decreasing faster than NO<sub>2</sub> in the three cities. At the curbside sites, this pattern is explained by the higher NO<sub>2</sub>:NO<sub>x</sub> emission ratios due to the introduction of some exhaust treatments for diesel vehicles (that convert NO to NO<sub>2</sub>) and the accelerated penetration of diesel PC (Grange et al., 2017). At urban background sites, the NO<sub>2</sub> concentrations are mainly controlled by the photochemical conversion of locally emitted NO to NO<sub>2</sub> rather than direct NO<sub>2</sub> emissions (Keuken et al., 2009; Anttila and Tuovinen, 2010). In urban atmospheres highly impacted by NO<sub>x</sub> emissions, a reduction in NO concentrations reduces the consumption of O<sub>3</sub> by titration (Monks et al., 2015) and, specifically for Europe, the regional background O<sub>3</sub> has been increasing (0.20–0.59 μg m<sup>-3</sup> yr<sup>-1</sup> for the annual mean in 1995–2014, Yan et al., 2018). As a consequence, more O<sub>3</sub> is available to oxidize NO to NO<sub>2</sub>, causing a steeper downward trend of NO concentrations than NO<sub>2</sub> at the urban background sites.

To facilitate the comparison of the concentration trends among sites with different pollution levels, changes were also expressed as percentage of variation per year over the period 1998–2017 (Fig. 2). The reductions in NO<sub>x</sub> concentrations in the urban background atmosphere were comparable in Copenhagen and Stockholm (−2.1 and −2.6% yr<sup>-1</sup>, respectively). In Denmark, the reduction in NO<sub>x</sub> emissions is due to the increasing use of catalysts in vehicles, and installation of low-NO<sub>x</sub>

burners and denitrifying units in power plants and district heating plants (Nielsen et al., 2019). In Sweden, the total decline in NO<sub>x</sub> emissions is linked to more stringent road transport emission standards, increased use of district heating and introduction of a NO<sub>x</sub> fee in 1992 for reducing industrial emissions (Swedish Environmental Protection Agency, 2020). Particularly, the former might be more relevant for Stockholm where road traffic is the dominant NO<sub>x</sub> source (Johansson et al., 2008). Note that changes in the urban atmosphere can be also affected by variations in the regional concentrations since they have non-negligible contributions (Ellermann et al., 2017; Krecl et al., 2011). The reduction in NO<sub>x</sub> concentrations in the urban background atmosphere of London was modest (−1.3% yr<sup>-1</sup>) compared to the other two cities.

Fig. 2 also shows that the negative trends of the NO<sub>x</sub> street increments in Copenhagen and Stockholm were even larger (−2.6 and −3.0% yr<sup>-1</sup>, respectively) than at the urban background sites. These large drops were attributed to variations in the traffic emissions over time, since neither the street canyons nor the adjacent areas underwent any changes in their configuration, and concentrations were already meteorologically normalized. In Denmark, the largest source of NO<sub>x</sub> emissions is road transport (30% in 2017), with a 65% decrease in the period 1998–2017 (mean of −3.2% yr<sup>-1</sup>) (Nielsen et al., 2019). Based on the emission inventories for Sweden in 1998 and 2017 (SCB, 2021), road traffic emissions were the main NO<sub>x</sub> sources and decreased 48.5% over the 20-year period, which corresponds to −2.4% yr<sup>-1</sup>. Thus, this national reduction in traffic emissions is in the same order of the reduction in concentrations found at the street canyon (−3.0% yr<sup>-1</sup>). In the case of London, the main emission source for NO<sub>x</sub> was road transport (49% in the year 2016 (Transport for London, 2016). Road transport also dominates the NO<sub>x</sub> emissions at national level in the UK (33% in 2017), with a reduction of 67% in the period 1998–2017 (DEFRA, 2020). This represents a reduction of −3.3% yr<sup>-1</sup> at UK level, which is far from the small street increment trend at Marylebone Road site (−0.2% yr<sup>-1</sup>). This large discrepancy could be explained by the use of emission inventories built with EF<sub>NO<sub>x</sub></sub> that largely underestimate the real emissions in the UK (Carslaw et al., 2011; Carslaw and Rhys-Tyler, 2013) and/or changes in the vehicle fleet composition for certain streets.

In relation to the NO<sub>2</sub> concentration trends, both urban background and curbside sites showed long-term improvements, but smaller for the latter where traffic emissions dominate. London presented the smallest decreases in concentration, with slight positive NO<sub>2</sub> street increment but

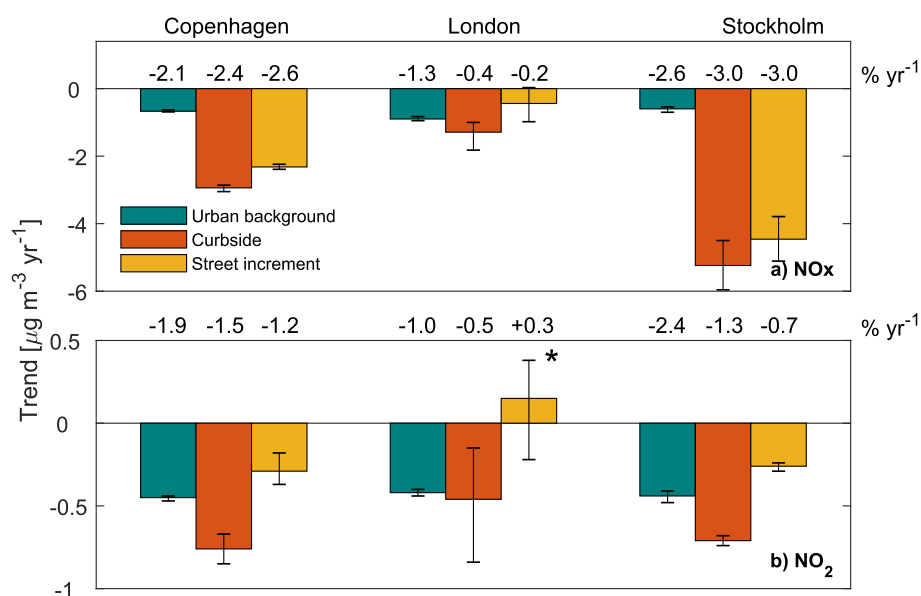


Fig. 2. Yearly trends (bar plots; in μg m<sup>-3</sup> yr<sup>-1</sup>) and relative changes (numbers; in % yr<sup>-1</sup>) in NO<sub>x</sub> (a) and NO<sub>2</sub> (b) concentrations for the three cities over the period 1998–2017, based on monthly mean changes in meteorologically normalized air pollutant concentrations at urban background and curbside sites, together with street increments. The error bars show the 95% confidence intervals of the trends. \*Indicates that the trend is not significant.

not statistically significant for the study period (1998–2017). The discussion on the  $\text{NO}_2:\text{NO}_x$  emission ratios is further developed in Section 3.2.

### 3.2. Trends in EF for the vehicle fleet

The annual evolutions of the  $\text{EF}_{\text{NO}_x}$  for the vehicle fleet at the three curbside sites over the study period are displayed in Fig. 3a–c. The grey shadows represent the 95% confidence interval of the mean, calculated using the monthly mean values for each year and site. In general, the decreasing trends observed at Jagtvej and Hornsgatan sites for the mixed fleet (Fig. 3 a,c) matched the temporal reduction in  $\text{EF}_{\text{NO}_x}$  for different vehicle categories/fuel, as reported by remote sensing studies conducted in European urban areas (Table 2). These results agree with the introduction of new technologies in the vehicle fleet to reduce air pollution emissions. However, the  $\text{EF}_{\text{NO}_x}$  pattern was rather constant at Marylebone Road over the period (Fig. 3b), and showed a larger monthly variability.

Inspecting the normalized  $\Delta\text{NO}_x$  trends (Fig. 3d–f), we can observe a clear resemblance between the  $\text{EF}_{\text{NO}_x}$  trends for Copenhagen and Stockholm (Fig. 3a, c). However, note that the  $\text{EF}_{\text{NO}_x}$  value was reported as the mean of the mixed fleet per vehicle whereas the normalized  $\Delta\text{NO}_x$  does not consider variations in traffic patterns (volume, speed, or vehicle type share). For example, the “bump” observed in the  $\text{EF}_{\text{NO}_x}$  time series at Hornsgatan site in the period 2011–2017 (Fig. 3c) coincided with the reduction in the total TR observed since January 2010, when a ban on studded tires was introduced for the wintertime and which remained over the years (Norman et al., 2016). The normalized  $\Delta\text{NO}_x$  was flat for the same period (Fig. 3f), suggesting that total  $\text{NO}_x$  emissions might have not changed, but increased per vehicle. We hypothesize that this increase in  $\text{EF}_{\text{NO}_x}$  for the mixed fleet at Hornsgatan site could have been caused by the introduction of buses fueled with 100% Rapeseed Methyl Ester (RME) in 2011, as part of the city of Stockholm’s strategy for running the entire bus fleet on renewable fuels and to comply with the Clean Vehicles Directive (2009/33/EC). Note that RME buses emit on average 2.5 times more  $\text{NO}_x$  than the diesel ones with similar buses engine and

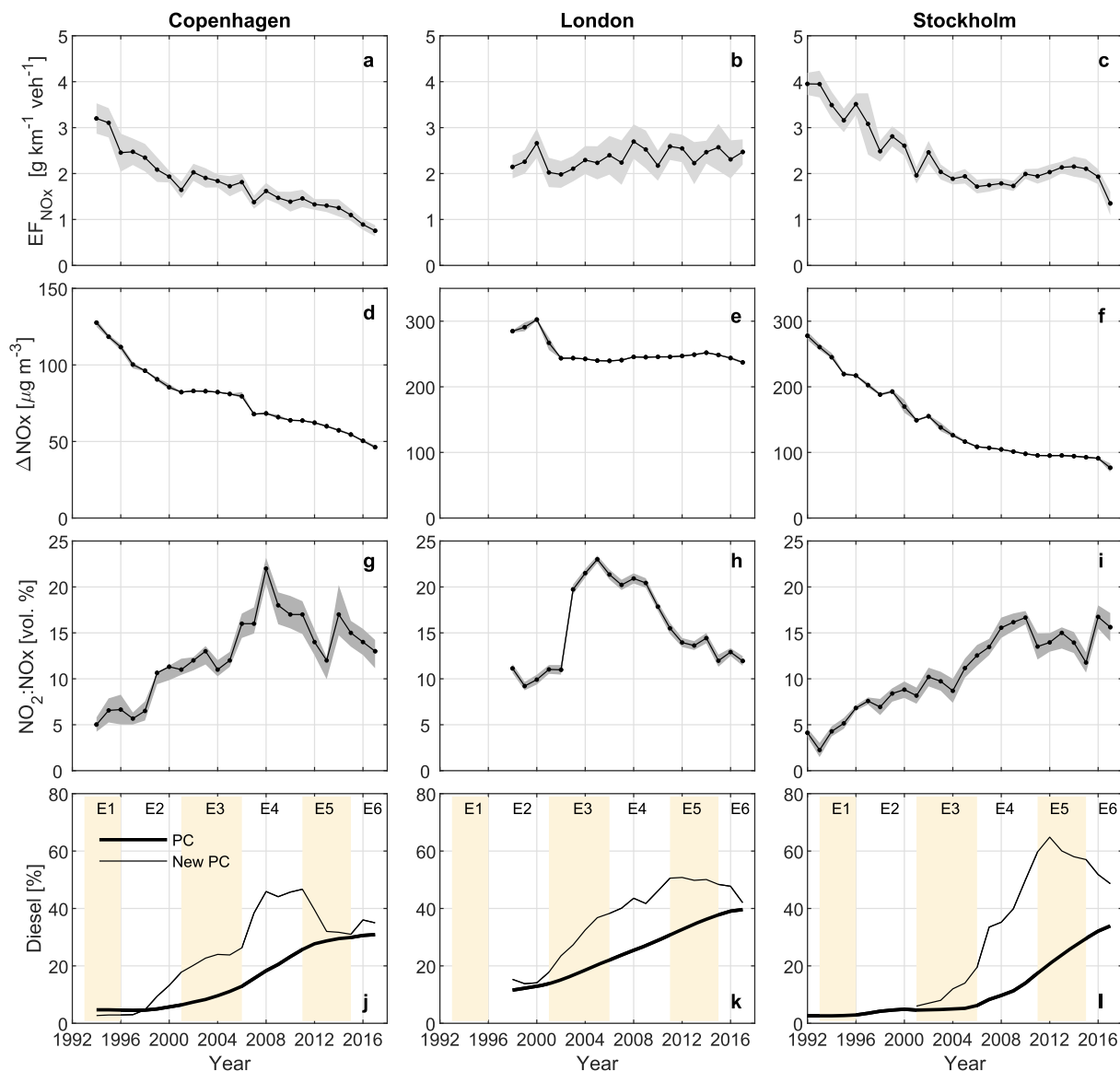


**Fig. 3.** a-c) Annual mean  $\text{EF}_{\text{NO}_x}$  for the vehicle fleet at the curbside sites, with the grey shadows representing the 95% confidence intervals. d-f) Annual mean  $\Delta\text{NO}_x$  concentrations (normalized) at curbside, together with the 95% confidence intervals. g-h) Annual  $\text{NO}_2:\text{NO}_x$  emission ratios at curbside with 95% confidence intervals. j-l) Diesel PC penetration in the national markets (International Council on Clean Transportation, 2018) expressed as percentages of all PC (thick black line) and new PC (thin black line), together with Euro standard registration dates (E1: Euro 1, E6: Euro 6).

after-treatment technology (Table S2, E5 and Selective Catalytic Reduction, SCR). In the year 2011, 10% of the public bus fleet was fueled with 100% RME (Johan Böhlin, personal communication, Feb. 2021), and the RME bus consumption doubled in 2014 (Clean Fleets, 2014). This information is consistent with the fast increase in RME sales in the Stockholm county in the period 2011–2017 (Stockholms stad, 2021). The reduction observed in  $EF_{NO_x}$  after the year 2015 might be mainly associated with the introduction of newer bus engines and/or cleaner exhaust after-treatment technologies for NO<sub>x</sub> emissions.

The  $\Delta NO_x$  trend at Marylebone Road demonstrates that, despite all the measures implemented for NO<sub>x</sub> control, the total emission remained stable since 2002. According to Font and Fuller (2016), the  $\Delta NO_x$  trends in London showed a large spatial heterogeneity in the period 2005–2014. They found that increasing  $\Delta NO_x$  trends were experienced on streets with increasing number of buses per day, such as Marylebone Road in 2010–2014. Conversely,  $\Delta NO_x$  reductions were associated with a lower traffic volume of buses and/or retrofitted buses with cleaner technologies (such as SCR + Diesel Particulate Filter, DPF, Carslaw et al., 2015).

The time evolution of the NO<sub>2</sub>:NO<sub>x</sub> emission ratios for the vehicle fleet is displayed in Fig. 3g–i for the three canyon sites. The interpretation is complex because the mean emission ratio for the whole fleet is influenced by the large variation observed with vehicle category/fuel and Euro standard stage (Table 2). The fraction of primary NO<sub>2</sub> emissions also depends on the exhaust after-treatment (particularly for buses, Table S2, Supplementary Material), vehicle mileage (Carslaw et al., 2019), mean VS (Grice et al., 2009), ambient temperature (Grange et al., 2019), and engine load (Carslaw et al., 2011; Carslaw and Rhys-Tyler, 2013). Moreover, differences in emission ratios vary considerably from manufacturer to manufacturer even for the same Euro standard stage and model year (Bernard et al., 2018; Carslaw et al., 2019).

Grange et al. (2017) showed a clear positive trend in annual mean NO<sub>2</sub>:NO<sub>x</sub> emission ratios for 61 European cities between 1995 and 2010. This trend can be attributed to the wide use of diesel oxidation catalysts (DOC) on PC—that target CO and hydrocarbons, but intentionally convert NO into NO<sub>2</sub> (Fiebig et al., 2014; Russell and Epling, 2011). Remote sensing studies confirm the increase of the NO<sub>2</sub>:NO<sub>x</sub> emission ratios with the introduction of DOC in E3 diesel PC (Table 2). The overall impact of these primary NO<sub>2</sub> emissions became important due to the dieselization of the European PC fleet, driven by improvements in fuel economy and supposed CO<sub>2</sub> emission reduction (Cames and Helmers, 2013).

This dieselization process was strong in the three countries (Fig. 3j–l) with the help of government incentives (Cames and Helmers, 2013). Even though the emission ratios are slightly higher for diesel LCV than for diesel PC for certain Euro stages (Table 2), diesel PC have become abundant at national and urban street levels in more recent times. For example, the shares of diesel PC and LCV in relation to the total fleet on Hornsgatan St. were 33 and 13% in 2017 vs. 17 and 11% in 2009. Note that when the shift towards the use of diesel fuel in PC at the expense of gasoline occurred, increasing NO<sub>2</sub>:NO<sub>x</sub> emission ratios were clearly observed at Jagtvej and Hornsgatan sites until 2008 and 2010, respectively (Fig. 3g,i). The decay in primary NO<sub>2</sub> emissions observed afterwards might be explained by the development of more efficient DOC systems by the car manufacturers (Carslaw et al., 2016; Carslaw et al., 2019). E6 standards introduced tighter limits for NO<sub>x</sub> emissions, and diesel PC were also equipped with NO<sub>x</sub> after-treatment systems that increased the NO<sub>2</sub>:NO<sub>x</sub> emission ratios again (Table 2, E6). Jagtvej and Hornsgatan experienced this increase in emission ratios but differences in time and magnitude might be explained by the composition of the diesel PC fleet per manufacturer group, given the large variations reported by Carslaw et al. (2019). Finally, the absolute NO<sub>x</sub> and NO<sub>2</sub> emissions remained low in the period matching the E6 stage, and reductions in  $\Delta NO_x$  and  $\Delta NO_2$  were found at Jagtvej (Fig. 2g,j) and Hornsgatan sites (Fig. 2i,l).

Note that certain particular characteristics of the vehicle fleet might

arise when analyzing the behavior of NO<sub>2</sub>:NO<sub>x</sub> emission ratios for individual cities and sites. Notably, Marylebone Road showed the maximum peak value (23 vol. %) in 2005 and dropped thereafter (Fig. 3h). This site was largely affected by changes in the urban bus engines and exhaust after-treatment technologies, since the number of buses operating on that street is high (e.g., 1473 buses per weekday in 2003). For example, the steep increase in ratios observed between 2002 and 2003 was attributed to the retrofitting program of London urban buses (E3 stage) with continuously regenerating particle traps (formed by a combination of DOC and DPF, Grange and Carslaw, 2019) and an increase in buses as part of the London congestion charge scheme (Givoni, 2012). The decline in ratios after 2008 was linked to the introduction of buses with newer and cleaner technologies and removal of old buses (Grange and Carslaw, 2019). The peak and decay of NO<sub>2</sub>:NO<sub>x</sub> at Marylebone Road were observed earlier than those in inner London (Carslaw et al., 2016) and we hypothesize that this shift might be due to the different implementation stages in the bus retrofitting programs and bus fleet renewal, depending on the analyzed street. Even though buses largely influence the emissions at Marylebone Road, the contribution of the diesel PC to the emission ratios cannot be ruled out because of their large number (Fig. 3k).

### 3.3. Comparison of $EF_{NO_x}$ at Hornsgatan with literature data

Fig. 4 shows the mean  $EF_{NO_x}$  for the mixed fleet at Hornsgatan site in the years 2009 and 2017 extracted from the EMEP and HBEFA databases, urban remote sensing studies (Table 2), and the results based on inverse modeling. Regardless of the method, lower  $EF_{NO_x}$  values were found in 2017 than in 2009, following the general trend of decreasing NO<sub>x</sub> emissions with the introduction of new engines and after-treatment systems.

For both years, the EMEP-based  $EF_{NO_x}$  presented the lowest values (0.73 and 0.51 g km<sup>-1</sup> veh<sup>-1</sup> in 2009 and 2017, respectively), whereas the results based on HBEFA and remote sensing studies were very similar (1.13 and 1.19 g km<sup>-1</sup> veh<sup>-1</sup> in 2009; 0.92 and 0.98 g km<sup>-1</sup> veh<sup>-1</sup> in 2017). This similarity might be explained by the update of the HBEFA database (V.3.3) with  $EF_{NO_x}$  of diesel PC for E4–E6 stages, considering new laboratory and real-world measurements (portable emission monitoring systems and remote sensing data), after compelling evidence that these EF were lower than in-use vehicles studies (Carslaw et al., 2011; Carslaw and Rhys-Tyler, 2013). The  $EF_{NO_x}$  presented in the EMEP guidebook were developed with the COPERT model, which has been

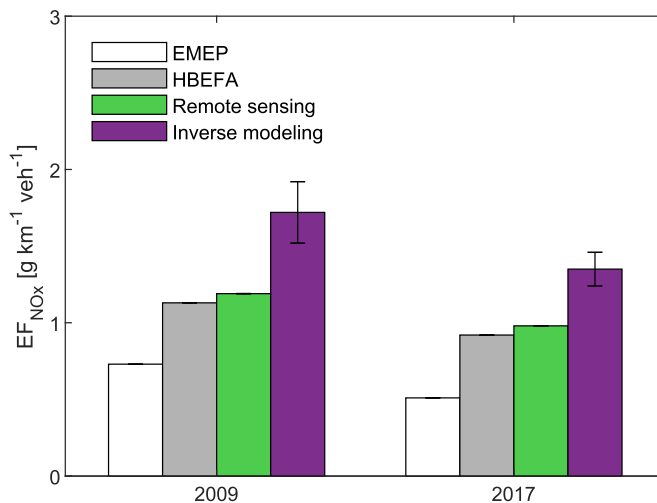


Fig. 4.  $EF_{NO_x}$  for the vehicle fleet at Hornsgatan site in the years 2009 and 2017 calculated using databases (EMEP and HBEFA), remote sensing studies (Table 2) and by inverse modeling. The error bars represent the 95% confidence intervals of the mean.

reported to predict lower NO<sub>x</sub> emissions than the HBEFA database under stop-and-go traffic conditions in cities, particularly for diesel vehicles (Borge et al., 2012). A recent UK study (Davison et al., 2021) also found that the national inventory—that heavily relies on the COPERT database—underestimates the NO<sub>x</sub> emissions from PC and LCV up to 47% in urban areas compared with emissions calculated with real-world EF<sub>NO<sub>x</sub></sub> from remote sensing studies.

The inverse modeling results presented the highest mean values for both years (1.72 and 1.35 g km<sup>-1</sup> veh<sup>-1</sup> in 2009 and 2017, respectively). The weighted EF<sub>NO<sub>x</sub></sub> calculations at Hornsgatan street using mean values per vehicle category from remote sensing data (Table 2) was a conservative approach. Considering the upper 95% confidence interval of EF<sub>NO<sub>x</sub></sub> for each vehicle category yielded weighted EF<sub>NO<sub>x</sub></sub> values much closer to those obtained with inverse modeling (1.69 and 1.23 g km<sup>-1</sup> veh<sup>-1</sup> in 2009 and 2017, respectively). Moreover, most of the remote sensing studies were conducted in the UK (Table 2), where ambient conditions and the mix of on-road vehicle manufacturers and engine sizes might be different from Hornsgatan St. Thus, all these factors could have contributed to the EF<sub>NO<sub>x</sub></sub> differences between inverse modeling and remote sensing methods.

### 3.4. Study strengths and limitations

As far as we know, this is the first study to analyze the trends of real-world EF<sub>NO<sub>x</sub></sub> for the vehicle fleet at the same locations over two decades. Previous studies analyzed NO<sub>x</sub> emission trends using only street increment concentrations as a proxy, or remote sensing measurements. Our approach (inverse modeling) presents advantageous features since: (i) we delivered EF<sub>NO<sub>x</sub></sub> rather than NO<sub>x</sub> street increments; this means that we addressed variations in traffic patterns that can largely influence emissions, and (ii) we assessed the overall effectiveness of policies for reducing the fleet emissions over a long time period. Although remote sensing studies provide individual EF<sub>NO<sub>x</sub></sub> for a large vehicle sample, they might not cover the entire fleet, particularly on busy roads with several lanes. Moreover, remote sensing field campaigns are usually short and traffic and ambient conditions might not be representative of the entire year.

This study was limited to the analysis of three paired sites because of the reduced availability of long-term measurements. Hence the transferability of the results to other streets in the same cities should be done cautiously, considering site-specific features and local traffic policies.

## 4. Conclusions

The Euro standard limits for new road vehicles have been successful in reducing NO<sub>x</sub> vehicle emissions in the studied sites and the ambient concentrations over time, except for Marylebone Road. This busy street canyon—which experienced an increase in bus traffic since 2003—masked the modest effects of the Euro standard limits on citywide road traffic emissions in London, as shown by the reduction in NO<sub>x</sub> concentrations in the urban background atmosphere. The NO<sub>2</sub>:NO<sub>x</sub> emission ratios showed a positive trend until 2008–2010, which was also reflected in the NO<sub>2</sub> ambient concentrations. This increase was associated with a strong dieselization process and the introduction of new after-treatment technologies that targeted the emission reduction of other species (greenhouse gases, carbon monoxide or particulate matter). Thus, while regulations on ambient concentrations of specific species have positive effects on human health, the overall outcomes should be considered before widely adopting them.

Our results suggest revising the low EF<sub>NO<sub>x</sub></sub> values presented in the EMEP guidebook for vehicle emissions, since they are used to compile official national inventories in Europe, estimate the exposures of population to air pollutants and of ecosystems to acidification and eutrophication. Finally, this work showed the relevance of long-term observations combined with dispersion modeling to detect trends, to assess the effectiveness of programs aimed at improving the urban air

quality, and to validate emission estimates based on models and laboratory tests.

## Supplementary Material

Details of air pollution sampling sites, traffic data, meteorological normalization of ambient concentrations, calculation of NO<sub>2</sub>:NO<sub>x</sub> ratios, determination of EF<sub>NO<sub>x</sub></sub> for the mixed fleet, partial dependence plots, and review of real-world EF<sub>NO<sub>x</sub></sub> for urban buses are available.

## Credit roles

**Patricia Krecl:** Conceptualization, Methodology, Formal analysis, Investigation, Data Curation, Visualization, Writing - Original Draft. **Roy M. Harrison:** Conceptualization, Formal analysis, Writing - Original Draft. **Christer Johansson:** Methodology, Formal analysis. **Admir Crésó Targino:** Formal analysis, Writing - Original Draft. **David C. Beddows:** Investigation. Software. **Thomas Ellerermann:** Investigation. **Camila Lara:** Visualization. **Matthias Ketzel:** Conceptualization, Methodology, Investigation, Writing - Original Draft.

## Declaration of competing interest

The authors declare that they have no known competing financial interests or personal relationships that could have appeared to influence the work reported in this paper.

## Acknowledgments

We acknowledge Lars Burman (Stockholm Environment and Health Administration) and Johan Böhlin (Stockholm Public Transport, SL) for detailed data and comments on Stockholm traffic emissions. P. Krecl's work was funded by grant 305145/2020-7 from the National Council for Scientific and Technological Development of Brazil (CNPq).

## Appendix A. Supplementary data

Supplementary data to this article can be found online at <https://doi.org/10.1016/j.envpol.2021.118105>.

## References

- Anttila, P., Tuovinen, J.P., 2010. Trends of primary and secondary pollutant concentrations in Finland in 1994-2007. *Atmos. Environ.* 44, 30–41. <https://doi.org/10.1016/j.atmosenv.2009.09.041>.
- Atkinson, R.W., Butland, B.K., Anderson, H.R., Maynard, R.L., 2018. Long-term Concentrations of Nitrogen Dioxide and Mortality. *Epidemiology*. <https://doi.org/10.1097/EDE.0000000000000847>.
- Berkowicz, R., 2000. OSPM: a parameterised street pollution model. *Environ. Monit. Assess.* 65, 323–331.
- Bernard, Y., Tietge, U., German, J., Muncrief, R., Foundation, F.I.A., Transportation, I.C., Ncap, G., Environment, T., Cities, C., 2018. Determination of Real-World Emissions from Passenger Vehicles Using Remote Sensing Data 31p. on C.
- Borge, R., de Miguel, I., de la Paz, D., Lumberras, J., Pérez, J., Rodríguez, E., 2012. Comparison of road traffic emission models in Madrid (Spain). *Atmos. Environ.* 62, 461–471. <https://doi.org/10.1016/j.atmosenv.2012.08.073>.
- Brown, J.S., 2015. Nitrogen dioxide exposure and airway responsiveness in individuals with asthma. *Inhal. Toxicol.* 27, 1–14. <https://doi.org/10.3109/08958378.2014.979960>.
- Burman, L., Elmgren, M., Norman, M., 2019. Fordonsmätningar På Hornsgatan År 2017.
- Cames, M., Helmers, E., 2013. Critical evaluation of the European diesel car boom - global comparison, environmental effects and various national strategies. *Environ. Sci. Eur.* 25, 1–22. <https://doi.org/10.1186/2190-4715-25-15>.
- Carlaw, D.C., Rhys-Tyler, G., 2013. New insights from comprehensive on-road measurements of NO<sub>x</sub>, NO<sub>2</sub> and NH<sub>3</sub> from vehicle emission remote sensing in London, UK. *Atmos. Environ.* 81, 339–347. <https://doi.org/10.1016/j.atmosenv.2013.09.026>.
- Carlaw, D.C., Ropkins, K., 2012. Openair - an R package for air quality data analysis. *Environ. Model. Software* 27 (28), 52–61. <https://doi.org/10.1016/j.envsoft.2011.09.008>.
- Carlaw, D.C., Beever, S.D., Tate, J.E., Westmoreland, E.J., Williams, M.L., 2011. Recent evidence concerning higher NO<sub>x</sub> emissions from passenger cars and light duty

- vehicles. *Atmos. Environ.* 45, 7053–7063. <https://doi.org/10.1016/j.atmosenv.2011.09.063>.
- Carslaw, D.C., Priestman, M., Williams, M.L., Stewart, G.B., Beevers, S.D., 2015. Performance of optimised SCR retrofit buses under urban driving and controlled conditions. *Atmos. Environ.* 105, 70–77. <https://doi.org/10.1016/j.atmosenv.2015.01.044>.
- Carslaw, D.C., Murrells, T.P., Andersson, J., Keenan, M., 2016. Have vehicle emissions of primary NO<sub>2</sub> peaked? *Faraday Discuss* 189, 439–454. <https://doi.org/10.1039/c5fd00162e>.
- Carslaw, D.C., Farren, N.J., Vaughan, A.R., Drysdale, W.S., Young, S., Lee, J.D., 2019. The diminishing importance of nitrogen dioxide emissions from road vehicle exhaust. *Atmos. Environ.* X 1, 100002. <https://doi.org/10.1016/j.aeoa.2018.100002>.
- Crippa, M., Janssens-Maenhout, G., Dentener, F., Guizzardi, D., Sindelarova, K., Muntean, M., Van Dingenen, R., Granier, C., 2016. Forty years of improvements in European air quality: regional policy-industry interactions with global impacts. *Atmos. Chem. Phys.* 16, 3825–3841. <https://doi.org/10.5194/acp-16-3825-2016>.
- Davison, J., Rose, R.A., Farren, N.J., Wagner, R.L., Murrells, T.P., Carslaw, D.C., 2021. Verification of a national emission inventory and influence of on-road vehicle manufacturer-level emissions. *Environ. Sci. Technol.* <https://doi.org/10.1021/acs.est.0c08363>.
- DEFRA, 2020. Statistical data set ENV01 - emissions of air pollutants. Annual update to tables on emissions of important air pollutants in the UK [WWW Document], n.d. URL: <https://www.gov.uk/government/statistical-data-sets/env01-emissions-of-air-pollutants>. accessed 3.27.21.
- EEA, 2019. European Union emission inventory report 1990–2017. EEA Report No 08/2019.
- Ellermann, T., Nygaard, J., Klønø Nøjgaard, J., Nordstrøm, C., Brandt, J., Christensen, J., Ketzel, M., Massling, A., Bossi, R., Solvang Jensen, S., 2017. AU Scientific Report from DCE-Danish Centre for Environment and Energy the Danish AIR QUALITY MONITORING PROGRAMME Annual Summary for 2017.
- EMEP/EEA, 2019. Air Pollutant Emission Inventory Guidebook 2019. EEA Report No 13/2019.
- EN14211, 2012. Ambient air — standard method for the measurement of the concentration of nitrogen dioxide and nitrogen monoxide by chemiluminescence (Brussels).
- EN14625, 2012. Ambient air - standard method for the measurement of the concentration of ozone by ultraviolet photometry. CEN. Brussels.
- European Commission, 2021. Emissions in the Automotive Sector [WWW Document]. URL: [https://ec.europa.eu/growth/sectors/automotive/environment-protection/emissions\\_en](https://ec.europa.eu/growth/sectors/automotive/environment-protection/emissions_en). accessed 3.27.21.
- European Environmental Agency, 2019. European Environmental Agency. Air Quality in Europe — 2019 Report.
- Fiebig, M., Wiertalla, A., Holderbaum, B., Kiesow, S., 2014. Particulate emissions from diesel engines: correlation between engine technology and emissions. *J. Occup. Med. Toxicol.* 9, 1–18. <https://doi.org/10.1186/1745-6673-9-6>.
- Fleets, Clean, 2014. Clean Buses — Experiences with Fuel and Technology. Options 1–42.
- Font, A., Fuller, G.W., 2016. Did policies to abate atmospheric emissions from traffic have a positive effect in London? *Environ. Pollut.* 218, 463–474. <https://doi.org/10.1016/j.envpol.2016.07.026>.
- Franco, V., Kousoulidou, M., Muntean, M., Ntziachristos, L., Hausberger, S., Dilara, P., 2013. Road vehicle emission factors development: a review. *Atmos. Environ.* 70, 84–97. <https://doi.org/10.1016/j.atmosenv.2013.01.006>.
- Fuzzi, S., Baltensperger, U., Carslaw, K., Deserai, S., Denier Van Der Gon, H., Facchini, M.C., Fowler, D., Koren, I., Langford, B., Lohmann, U., Nemitz, E., Pandis, S., Riipinen, I., Rudich, Y., Schaap, M., Slowik, J.G., Spracklen, D.V., Vignati, E., Wild, M., Williams, M., Gilardoni, S., 2015. Particulate matter, air quality and climate: lessons learned and future needs. *Atmos. Chem. Phys.* 15, 8217–8299. <https://doi.org/10.5194/acp-15-8217-2015>.
- Ghaffarpassand, O., Beddows, D.C.S., Ropkins, K., Pope, F.D., 2020. Real-world assessment of vehicle air pollutant emissions subset by vehicle type, fuel and EURO class: new findings from the recent UK EDAR field campaigns, and implications for emissions restricted zones. *Sci. Total Environ.* 734, 139416. <https://doi.org/10.1016/j.scitotenv.2020.139416>.
- Givoni, M., 2012. Re-assessing the results of the London congestion charging scheme. *Urban Stud.* 49, 1089–1105. <https://doi.org/10.1177/0042098011417017>.
- Grange, S.K., Carslaw, D.C., 2019. Using meteorological normalisation to detect interventions in air quality time series. *Sci. Total Environ.* 653, 578–588. <https://doi.org/10.1016/j.scitotenv.2018.10.344>.
- Grange, S.K., Lewis, A.C., Moller, S.J., Carslaw, D.C., 2017. Lower vehicular primary emissions of NO<sub>2</sub> in Europe than assumed in policy projections. *Nat. Geosci.* 10, 914–918. <https://doi.org/10.1038/s41561-017-0009-0>.
- Grange, S.K., Farren, N.J., Vaughan, A.R., Rose, R.A., Carslaw, D.C., 2019. Strong temperature dependence for light-duty diesel vehicle NO<sub>x</sub> emissions. *Environ. Sci. Technol.* 53, 6587–6596.
- Grennfelt, P., Englyerd, A., Forsius, M., Hov, Ø., Rodhe, H., Cowling, E., 2020. Acid rain and air pollution: 50 years of progress in environmental science and policy. *Ambio* 49, 849–864. <https://doi.org/10.1007/s13280-019-01244-4>.
- Grice, S., Stedman, J., Kent, A., Hobson, M., Norris, J., Abbott, J., Cooke, S., 2009. Recent trends and projections of primary NO<sub>2</sub> emissions in Europe. *Atmos. Environ.* 43, 2154–2167. <https://doi.org/10.1016/j.atmosenv.2009.01.019>.
- Harrison, R.M., Beddows, D.C.S., Dall'Osto, M., 2011. PMF analysis of wide-range particle size spectra collected on a major highway. *Environ. Sci. Technol.* 45, 5522–5528. <https://doi.org/10.1021/es201998m>.
- International Council on Clean Transportation, 2018. European Vehicle Market Statistics. Pocketbook, 2018/19 63.
- Johansson, C., Andersson, C., Bergström, R., Krecel, P., 2008. ITM-rapport 175.
- Kakosimos, K.E., Hertel, O., Ketzel, M., Berkowicz, R., 2010. Operational Street Pollution Model (OSPM) - a review of performed application and validation studies, and future prospects. *Environ. Chem.* 7, 485–503. <https://doi.org/10.1071/EN10070>.
- Kamińska, J.A., 2019. A random forest partition model for predicting NO<sub>2</sub> concentrations from traffic flow and meteorological conditions. *Sci. Total Environ.* 651, 475–483. <https://doi.org/10.1016/j.scitotenv.2018.09.196>.
- Ketzel, M., Wählin, P., Berkowicz, R., Palmgren, F., 2003. Particle and trace gas emission factors under urban driving conditions in Copenhagen based on street and roof-level observations. *Atmos. Environ.* 37, 2735–2749. [https://doi.org/10.1016/S1352-2310\(03\)00245-0](https://doi.org/10.1016/S1352-2310(03)00245-0).
- Keuken, M., Roemer, M., van den Elshout, S., 2009. Trend analysis of urban NO<sub>2</sub> concentrations and the importance of direct NO<sub>2</sub> emissions versus ozone/NO<sub>x</sub> equilibrium. *Atmos. Environ.* 43, 4780–4783. <https://doi.org/10.1016/j.atmosenv.2008.07.043>.
- Krecel, P., Targino, A.C., Johansson, C., 2011. Spatiotemporal distribution of light-absorbing carbon and its relationship to other atmospheric pollutants in Stockholm. *Atmos. Chem. Phys.* 11, 11553–11567. <https://doi.org/10.5194/acp-11-11553-2011>.
- Krecel, P., Targino, A.C., Johansson, C., Ström, J., 2015. Characterisation and source apportionment of submicron particle number size distributions in a busy street canyon. *Aerosol Air Qual. Res.* 15, 220–233. <https://doi.org/10.4209/aaqr.2014.06.0108>.
- Krecel, P., Johansson, C., Targino, A.C., Ström, J., Burman, L., 2017. Trends in black carbon and size-resolved particle number concentrations and vehicle emission factors under real-world conditions. *Atmos. Environ.* 165, 155–168. <https://doi.org/10.1016/j.atmosenv.2017.06.036>.
- Krecel, P., Targino, A.C., Landi, T.P., Ketzel, M., 2018. Determination of black carbon, PM<sub>2.5</sub>, particle number and NO<sub>x</sub> emission factors from roadside measurements and their implications for emission inventory development. *Atmos. Environ.* 186, 229–240. <https://doi.org/10.1016/j.atmosenv.2018.05.042>.
- Laña, I., Del Ser, J., Padró, A., Vélez, M., Casanova-Mateo, C., 2016. The role of local urban traffic and meteorological conditions in air pollution: a data-based case study in Madrid, Spain. *Atmos. Environ.* 145, 424–438. <https://doi.org/10.1016/j.atmosenv.2016.09.052>.
- Liefferink, D., Arts, B., Kamstra, J., Ooijselaar, J., 2009. Leaders and laggards in environmental policy: a quantitative analysis of domestic policy outputs. *J. Eur. Publ. Pol.* 16, 677–700. <https://doi.org/10.1080/13501760902983283>.
- Liu, Q., Hallquist, Å.M., Fallgren, H., Jerksjö, M., Jutterström, S., Salberg, H., Hallquist, M., Le Breton, M., Pei, X., Pathak, R.K., Liu, T., Lee, B., Chan, C.K., 2019. Roadside assessment of a modern city bus fleet: gaseous and particle emissions. *Atmos. Environ.* X 3, 100044. <https://doi.org/10.1016/j.aeoa.2019.100044>.
- Malley, C.S., Von Schneidmesser, E., Moller, S., Braban, C.F., Kevin Hicks, W., Heal, M. R., 2018. Analysis of the distributions of hourly NO<sub>2</sub> concentrations contributing to annual average NO<sub>2</sub> concentrations across the European monitoring network between 2000 and 2014. *Atmos. Chem. Phys.* 18, 3563–3587. <https://doi.org/10.5194/acp-18-3563-2018>.
- McDuffie, E.E., Smith, S.J., O'Rourke, P., Tibrewal, K., Venkataraman, C., Marais, E.A., Zheng, B., Crippa, M., Brauer, M., Martin, R.V., 2020. A global anthropogenic emission inventory of atmospheric pollutants from sector- and fuel-specific sources (1970–2017): an application of the Community Emissions Data System (CEDS). *Earth Syst. Sci. Data* 12, 3413–3442. <https://doi.org/10.5194/essd-12-3413-2020>.
- Monks, P.S., Archibald, A.T., Colette, A., Cooper, O., Coyle, M., Derwent, R., Fowler, D., Granier, C., Law, K.S., Mills, G.E., Stevenson, D.S., Tarasova, O., Thouret, V., Von Schneidmesser, E., Sommariva, R., Wild, O., Williams, M.L., 2015. Tropospheric ozone and its precursors from the urban to the global scale from air quality to short-lived climate forcer. *Atmos. Chem. Phys.* 15, 8889–8973. <https://doi.org/10.5194/acp-15-8889-2015>.
- Nathan, C., Cunningham-Bussell, A., 2013. Beyond oxidative stress: an immunologist's guide to reactive oxygen species. *Nat. Rev. Immunol.* 13, 349–361. <https://doi.org/10.1038/nri3423>.
- Nielsen, O.-K., Plejdrup, M.S., Winther, M., Mikkelsen, M.H., Nielsen, M., Gyldenkarne, S., Fauser, P., Albrektsen, R., Hjelgaard, K.H., Bruun, H.G., Thomsen, M., 2019. Annual Danish Informative Inventory Report to UNECE. Emission Inventories from the Base Year of the Protocols to Year 2017.
- Norman, M., Sundvor, I., Denby, B.R., Johansson, C., Gustafsson, M., Blomqvist, G., Janhäll, S., 2016. Modelling road dust emission abatement measures using the NORTRIP model: vehicle speed and studded tyre reduction. *Atmos. Environ.* 134, 96–108. <https://doi.org/10.1016/j.atmosenv.2016.03.035>.
- Olstrup, H., Forsberg, B., Orru, H., Nguyen, H., Molnár, P., Johansson, C., 2018. Trends in air pollutants and health impacts in three Swedish cities over the past three decades. *Atmos. Chem. Phys.* 18, 15705–15723. <https://doi.org/10.5194/acp-18-15705-2018>.
- Ottosen, T.B., Kakosimos, K.E., Johansson, C., Hertel, O., Brandt, J., Skov, H., Berkowicz, R., Ellermann, T., Jensen, S.S., Ketzel, M., 2015. Analysis of the impact of inhomogeneous emissions in the operational street pollution model (OSPM). *Geosci. Model Dev. (GMD)* 8, 3231–3245. <https://doi.org/10.5194/gmd-8-3231-2015>.
- Palmgren, F., Berkowicz, R., Ziv, A., Hertel, O., 1999. Actual car fleet emissions estimated from urban air quality measurements and street pollution models. *Sci. Total Environ.* 235, 101–109. [https://doi.org/10.1016/S0048-9697\(99\)00196-5](https://doi.org/10.1016/S0048-9697(99)00196-5).
- Peel, J.L., Haeuber, R., Garcia, V., Russell, A.G., Neas, L., 2013. Impact of nitrogen and climate change interactions on ambient air pollution and human health. *Biogeochemistry* 114, 121–134. <https://doi.org/10.1007/s10533-012-9782-4>.
- Russell, A., Epling, W.S., 2011. Diesel oxidation catalysts. *Catal. Rev. Sci. Eng.* 53, 337–423. <https://doi.org/10.1080/01614940.2011.596429>.

- SCB, 2021. Emissions of Air Pollutants from Domestic Transport by Mode of Transport. Year 1990 – 2019 [WWW Document]. [https://www.statistikdatabasen.scb.se/pxweb/en/ssd/START\\_MI\\_MI0108/MI0108InTransp/](https://www.statistikdatabasen.scb.se/pxweb/en/ssd/START_MI_MI0108/MI0108InTransp/). accessed 3.27.21.
- Snell, J., Birkes, D., Dodge, Y., 1996. Alternative methods of regression. *J. Roy Statist. Soc. Ser. A Statist. Soc.* Wiley-Intersci. <https://doi.org/10.2307/2983483>. Wiley Ser. ed.
- Proportion of environmental fuel in the Stockholm county [WWW Document], n.d. URL Stockholm stad. <http://miljobarometern.stockholm.se/miljomal/miljoprogram-2016-2019/miljoanpassade-transporter/minskat-fossilberoende/andel-miljobransle-i-stockholms-lan/rapsbransle/table/>. accessed 3.27.21.
- Swedish Environmental Protection Agency, 2020. Informative Inventory Report Sweden 2020.
- Transport for London, 2016. London Atmospheric Emissions Inventory. LAEI [WWW Document], n.d. URL <https://data.london.gov.uk/dataset/london-atmospheric-emissions-inventory-laei-2016>. accessed 3.27.21.
- Yan, Y., Pozzer, A., Ojha, N., Lin, J., Lelieveld, J., 2018. Analysis of European ozone trends in the period 1995-2014. *Atmos. Chem. Phys.* 18, 5589–5605. <https://doi.org/10.5194/acp-18-5589-2018>.
- Zhou, L., Liu, Q., Lee, B.P., Chan, C.K., Hallquist, Å.M., Sjödin, Å., Jerksjö, M., Salberg, H., Wängberg, I., Hallquist, M., Salvador, C.M., Gaita, S.M., Mellqvist, J., 2020. A transition of atmospheric emissions of particles and gases from on-road heavy-duty trucks. *Atmos. Chem. Phys.* 20, 1701–1722. <https://doi.org/10.5194/acp-20-1701-2020>.